

Biophysical Studies on the Effect of the 13 Position Substitution of the Anticancer Alkaloid Berberine on Its DNA Binding

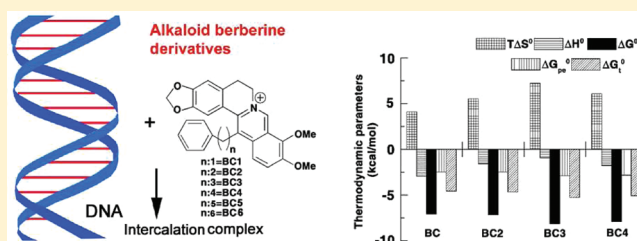
Debipreeta Bhowmik,[†] Maidul Hossain,[†] Franco Buzzetti,[‡] Rosaria D'Auria,[‡] Paolo Lombardi,[‡] and Gopinatha Suresh Kumar^{*,†}

[†]Biophysical Chemistry Laboratory, Chemistry Division, CSIR-Indian Institute of Chemical Biology, Kolkata 700 032, India

[‡]Naxospharma srl, Via G. Di Vittorio, 70 - 20026 - Novate Milanese (MI), Italy

S Supporting Information

ABSTRACT: The structural effects and thermodynamics of the DNA binding of six berberine analogues with alkyl chains of varying length and a terminal phenyl group at the C-13 position were investigated. All the analogues bound DNA noncooperatively in contrast to the cooperative binding of berberine. The binding affinity was higher and the effect of the chain length was only up to $(\text{CH}_2)_3$, after which the binding affinity decreased slightly. Intercalative binding with strong stabilization of the DNA helix was revealed. Binding resulted in the weakening of the base stacking with moderate conformational changes within the B-form. The binding was entropy driven in each case, the entropy contribution to the free energy increasing with the chain length up to the threshold $(\text{CH}_2)_3$. The complexation was dominated by nonpoelectrolytic forces in each case; polyelectrolytic forces contributed only a quarter to the total free energy at 50 mM $[\text{Na}^+]$. Overall, the phenylalkyl substitution at the C-13 position considerably enhanced the DNA binding and was highest for the analogue with $(\text{CH}_2)_3$. Structural and thermodynamic data on the DNA binding aspects of the substituted berberines are presented in comparison with berberine.



1. INTRODUCTION

Isoquinoline alkaloids represent a group of natural products extensively distributed in the plant kingdom and exhibiting a myriad of therapeutic activities.¹ Berberine (Figure 1A), an

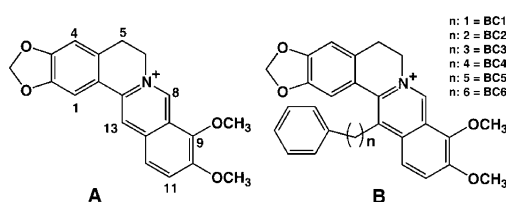


Figure 1. Chemical structures of (A) berberine and (B) berberine analogues.

ideal representative of this group, has attracted remarkable attention for its extensive use in biomedical research with multiple pharmacological effects.² Its antiinflammatory effect and antimicrobial activities have been demonstrated against many species.³ The alkaloid has been reported to exhibit antiproliferative activity in vitro and induced apoptosis/necrosis in several cell lines tested.⁴ A number of reports on the anticancer properties of berberine against a variety of different cell lines and operating through various mechanisms are reported in the literature.⁵ Although the precise molecular basis of the biological activities is still debated, emerging new information continues to build up data that is exploitable for clinical applications.

The anticancer activity of berberine appears to derive from its ability to form strong complexes with nucleic acids, induce DNA damage, and exert related effects such as telomerase inhibition, topoisomerase poisoning, and inhibition of gene transcription.⁶ Consequently, extensive studies on the mode, mechanism, and base pair specificity of the binding of berberine were reported^{6–8} from our laboratory and many other laboratories. It has now become clear that the alkaloid is an adenine–thymine base pair specific DNA binding agent.⁷ However, there was considerable controversy over its binding mode with conflicting reports of partial intercalation and groove binding model of interactions.⁸ Very recently, the crystal structure of berberine-d(CGTACG)₂ complex has been solved by Gratteri and colleagues,⁹ confirming a nonclassical intercalation model for its DNA binding, thus settling the long-standing controversy and confirming our suggestion from spectroscopy.^{7a}

Berberine has emerged as an attractive lead compound for the development of functional DNA binding drugs. It has an extended π delocalized system with a positive charge on the nitrogen atom. Hydrogen atoms on the basic core are replaced by methylenedioxy and methoxy groups. Analysis of the structure–activity relationship of berberine has suggested that positions 9 and 13 are critical for topoisomerase inhibition and

Received: October 20, 2011

Revised: January 17, 2012

Published: January 25, 2012

quadruplex binding.¹⁰ Furthermore, derivatives of berberine with substitutions at the 9 and 13 positions have been shown to have better anticancer activity in human cancer cells¹¹ besides enhanced antifungal and antibacterial activities.¹² Many studies on the DNA binding of the 9-substituted berberines revealed enhanced binding¹³ and also induction of novel self-structure formations in single stranded poly(A).¹⁴ Similarly, many 13-alkyl substituted berberines were shown to have better biological activity¹⁵ and quadruplex stabilizing ability¹⁶ than the parent berberine. Nevertheless, detailed duplex DNA binding studies were not performed on these derivatives. Therefore, we studied the DNA binding activity of a series of 13 substituted berberines (Figure 1B) carrying an alkyl chain of varying length with a terminal phenyl group. The assumption was that elucidation of the DNA binding activity of these berberine analogues might provide a new way of seeking other pharmacological activities of these compounds. We present here the results of spectroscopic and calorimetric studies that give specific and interesting insights into the effect of the alkyl chain length on the DNA binding aspects.

2. MATERIALS AND METHODS

2.1. Materials. Berberine chloride (BC) and calf thymus (CT) DNA (highly polymerized, sodium salt, type XI, 42% GC content) were obtained from Sigma-Aldrich Corporation (St. Louis, MO, USA). BC was used as received. The DNA sample was sonicated in a Labsonic sonicator (B. Brown, Germany) to molecular weights of $1-2 \times 10^5$ Da and was dialyzed under sterile conditions at 5 °C into the experimental buffer. The ratio of the $A_{260/280}$ for the DNA gave values between 1.8 and 1.9, indicating the protein free nature of the sample. A molar extinction coefficient (ϵ) value of $13\,200\text{ M}^{-1}\text{ cm}^{-1}$ (in base pairs) at 260 nm was used for estimating the concentration of the aqueous DNA solution. The 13-phenylalkyl berberine analogues were designed, synthesized, and characterized by Naxospharma, Italy.¹⁷ They were fairly soluble in aqueous buffers, and hence their solutions were freshly prepared each day and kept protected in the dark until use. The concentration of berberine was determined by an ϵ value of $22\,500\text{ M}^{-1}\text{ cm}^{-1}$ at 345 nm and that of the 13-analogues using a common molar extinction coefficient value of $19\,500\text{ M}^{-1}\text{ cm}^{-1}$ at 339 nm. No deviation from Beer's law was observed in the concentration range used in this study. All experiments were conducted in citrate-phosphate (CP) buffer of pH 7.0, containing 5 mM Na_2HPO_4 , the pH being adjusted with citric acid. Measurements of pH were made on a Sartorius PB-11 high precision bench pH meter (Sartorius GmbH, Germany) with an accuracy of ± 0.01 units. Glass distilled deionized water and analytical grade reagents were used throughout. All buffer solutions were filtered through Millipore filters (Millipore, India Pvt. Ltd., Bangalore, India) of 0.22 μm .

2.2. Binding Studies by Spectroscopy. Absorbance spectral studies were performed on a Jasco V660 double beam double monochromator spectrophotometer (Japan International Co., Hachioji, Japan) at 20 ± 0.5 °C using the methodology of Chaires¹⁸ and described in detail by us previously.¹⁹ For titration, matched quartz cells (Hellma, Germany) of 1 cm path length were used. Briefly, a known concentration of the DNA solution was kept in the sample and reference cells and small aliquots of a known concentration of the alkaloid/alkaloid analogue solution were titrated into the sample cell. After each addition, the solution was thoroughly mixed and allowed to re-equilibrate for at least 10 min before

noting the absorbance at the wavelength maximum and the isosbestic point. The data obtained from these titrations were used for constructing Scatchard plots.

Steady state fluorescence measurements were performed on either a Shimadzu RF 5301 PC (Shimadzu Corporation, Kyoto, Japan) or a Hitachi F4010 (Hitachi Ltd., Tokyo, Japan) fluorescence spectrometer in fluorescence free quartz cells of 1 cm path length as described previously.²⁰ The excitation wavelength for berberine and its analogues was 350 nm. Since emission spectra of the complexes were in a region far away from the excitation wavelength, no overlap of the bands was observed in any case. All measurements were performed keeping excitation and emission band passes of 5 nm. The sample temperature was maintained at 20 ± 1.0 °C using an Eyela Uni Cool USS water bath (Tokyo Rikakikai Co. Ltd., Tokyo, Japan). No deviation from Beer's law was observed in the concentration range employed in this study.

The amount of free and bound alkaloid/alkaloid analogue was determined as follows. In absorption spectroscopy, following each addition of the alkaloid to the DNA solution (50 μM), the total alkaloid concentration present was calculated as $C_t = A_{\text{iso}}/\epsilon_{\text{iso}}$ from the absorbance at the respective isosbestic point (A_{iso}), where ϵ_{iso} is the molar extinction coefficient at the isosbestic point. The expected absorbance (A_{exp}) at the wavelength maximum was calculated using the relation $A_{\text{exp}} = C_t \epsilon_{\text{max}}$, where ϵ_{max} is the molar extinction coefficient at the wavelength maximum. The difference in A_{exp} and the observed absorbance (A_{obsd}) was then used to calculate the amount of bound alkaloid as $C_b = A/\Delta\epsilon = (A_{\text{exp}} - A_{\text{obsd}})/(\epsilon_f - \epsilon_b)$. The concentration of the free alkaloid was determined by the difference $C_f = C_t - C_b$. The extinction coefficient of the completely bound alkaloid was determined by adding a known quantity of the alkaloid to a large excess of DNA and on the assumption of total binding, $\epsilon_b = A_{\text{max}}/C_t$. Alternatively, the absorbance of a known quantity of the alkaloid was monitored at the wavelength maximum while adding known amounts of DNA until no further change in absorbance was observed. Both of these methods gave identical values within experimental error. In fluorescence, C_b was calculated from the relation $C_b = C_t(I - I_o)/(V_o - 1)I_o$, where C_t is the total alkaloid concentration, I is the observed fluorescence intensity, I_o is the fluorescence intensity of identical concentration of the alkaloid in the absence of DNA, and V_o is the experimentally determined ratio of the fluorescence intensity of totally bound alkaloid to that of the free alkaloid. Free alkaloid concentrations (C_f) were obtained from the relationship $C_t = C_b + C_f$. The binding ratio r is defined as $r = C_b/[\text{DNA}]_{\text{total}}$.

2.3. Analysis of the Binding Data. Scatchard plots (r/C_f versus r) were constructed from the binding data obtained from spectrophotometric and spectrofluorimetric titrations. The Scatchard isotherms with positive slope at low r values were analyzed using the following McGhee–von Hippel equation for cooperative binding.²¹

$$\frac{r}{C_f} = K_f(1 - nr) \left(\frac{(2\omega + 1)(1 - nr) + (r - R)}{2(\omega - 1)(1 - nr)} \right)^{(n-1)} \left(\frac{1 - (n+1)r + R}{2(1 - nr)} \right)^2 \quad (1)$$

where $R = \{[1 - (n+1)r]^2 + 4\omega r(1 - nr)\}^{1/2}$.

Scatchard plots with negative slopes at low r values were analyzed by the noncooperative binding model of McGhee and von Hippel as per the following equation

$$r/C_f = K_i(1 - nr)[(1 - nr)/(1 - (n - 1)r)]^{(n-1)} \quad (2)$$

Here, K_i is the intrinsic binding constant to an isolated binding site, n is the number of base pairs excluded by the binding of a single alkaloid molecule, and ω is the cooperativity factor. All the binding data were analyzed using the Origin 7.0 software (Origin Laboratories, Northampton, MA, USA) that determines the best-fit parameters of K_i , n , and ω to eq 1 and of K_i and n to eq 2.

2.4. Stoichiometry of Binding: Job Plot. The continuous variation method of Job²² was employed to determine the binding stoichiometry in each case from fluorescence spectroscopy. Steady state fluorescence measurements were performed in fluorescence free quartz cells of 1 cm path length as described previously.^{20a,23} All the measurements were performed at a constant temperature of 20 ± 1 °C under conditions of continuous stirring. Uncorrected fluorescence spectra were recorded. The fluorescence signal was recorded for solutions where the concentrations of both DNA and the alkaloid were varied while the sum of their concentrations was kept constant. The difference in fluorescence intensity (ΔF) of the alkaloids in the absence and presence of DNA was plotted as a function of the input mole fraction of each alkaloid. The break point in the resulting plot corresponds to the mole fraction of the bound alkaloid in the complex. The stoichiometry was obtained in terms of DNA–alkaloid $[(1 - \chi_{\text{alkaloid}})/\chi_{\text{alkaloid}}]$, where χ_{alkaloid} denotes the mole fraction of the respective alkaloid. The results reported are averages of at least three experiments.

2.5. Fluorescence Quenching Studies. Quenching studies were carried out with the anionic quencher $[\text{Fe}(\text{CN})_6]^{4-}$. Quenching experiments were performed by mixing, in different ratios, two solutions, one containing KCl and the other containing $\text{K}_4[\text{Fe}(\text{CN})_6]$, in addition to the normal buffer components, at a fixed total ionic strength. Experiments were performed at a constant P/D (DNA base pair/alkaloid molar ratio), monitoring fluorescence intensity as a function of the increasing concentration of ferrocyanide ion as described in detail previously.²⁴ At least four measurements were taken for each set and averaged out. The data were plotted as Stern–Volmer plots of relative fluorescence intensity (F_0/F) versus $[\text{Fe}(\text{CN})_6]^{4-}$.

2.6. Hydrodynamic Studies. The viscosity of the DNA–alkaloid complexes was determined by measuring the time needed to flow through a Cannon–Manning semi micro size 75 capillary viscometer (Cannon Instruments Company, State College, PA, USA) that was submerged in a thermostatted bath (20 ± 1 °C) as reported previously.^{20b} Flow times were measured in triplicate to an accuracy of ± 0.01 s with an electronic stopwatch - Casio Model HS-30W (Casio Computer Co. Ltd., Tokyo, Japan). Relative viscosities for DNA either in the presence or absence of the alkaloids were calculated from the relation

$$\eta'_{\text{sp}}/\eta_{\text{sp}} = \{(t_{\text{complex}} - t_0)/t_0\}/\{(t_{\text{control}} - t_0)/t_0\} \quad (3)$$

where η'_{sp} and η_{sp} are specific viscosities of the alkaloid–DNA complex and the DNA, respectively; t_{complex} , t_{control} , and t_0 are the average flow times for the DNA–alkaloid complex, free

DNA, and buffer, respectively. The relative increase in length of DNA, L/L_0 , is obtained from the corresponding increase in relative viscosity using the following equation²⁵

$$L/L_0 = (\eta/\eta_0)^{1/3} = 1 + \beta r \quad (4)$$

where L and L_0 are the contour lengths of DNA in the presence and absence of the alkaloid, η and η_0 are the corresponding values of intrinsic viscosity (approximated by the reduced viscosity $\eta = \eta_{\text{sp}}/C$, where C is the DNA concentration), and β is the slope of the plot of L/L_0 versus r .

2.7. Optical Thermal Melting and Differential Scanning Calorimetry. Absorbance versus temperature curves (melting profiles) of DNA and DNA–alkaloid complexes were measured on the Shimadzu Pharmaspec 1700 unit (Shimadzu Corporation) equipped with the peltier controlled TMSPC-8 model accessory as described earlier.^{20a,26} In a typical experiment, the DNA sample (50 μM) was mixed with varying concentrations of the alkaloid under study and the mixture was heated at a rate of 0.5 °C/min, continuously monitoring the absorbance change at 260 nm. T_m is the midpoint of the melting transition as determined by the maxima of the first derivative plots.

Excess heat capacities as a function of temperature were measured on a Microcal VP-differential scanning calorimeter (DSC) (MicroCal, Inc., Northampton, MA, USA) as described previously.^{20a,23} In a series of DSC scans, both the cells were loaded at first with the buffer, equilibrated at 35 °C for 15 min, and scanned from 35 to 110 °C at a rate of 50 °C/h. The buffer scans were repeated until reproducible (noise specification <0.5 $\mu\text{cal}/^\circ\text{C}$ and repeatability specification <1.3 $\mu\text{cal}/^\circ\text{C}$). On cooling, the sample cell was rinsed, loaded with DNA followed by the DNA–alkaloid complex (molar ratio = 0.8), and scanned in the range 35–110 °C. Each experiment was repeated twice with separate fillings. The DSC thermograms of excess heat capacity versus temperature were analyzed using the Origin 7.0 software. The area under the experimental heat capacity (C_p°) curves was used to determine the calorimetric transition enthalpy (ΔH_{cal}) given by the equation

$$\Delta H_{\text{cal}} = \int C_p^\circ dT \quad (5)$$

where T is the absolute scale temperature in kelvins. This calorimetrically determined enthalpy is model-independent and thus unrelated to the nature of the transition. The temperature at which excess heat capacity is at a maximum defines the transition temperature (T_m). The model-dependent van't Hoff enthalpy (ΔH_v) was obtained by shape analysis of the calorimetric data, and the cooperativity factor was obtained from the ratio $(\Delta H_{\text{cal}}/\Delta H_v)$.^{20a,23}

2.8. Isothermal Titration Calorimetry. All isothermal titration calorimetry experiments were performed using a MicroCal VP-ITC unit (MicroCal, Inc., Northampton, MA, USA) using protocols developed in our laboratory and described in detail previously.^{20a,23,24a,26} Briefly, aliquots of degassed BC and BC analogue solutions were injected from a rotating syringe (290 rpm) into the isothermal sample chamber containing the DNA solution (1.4235 mL). Corresponding control experiments to determine the heat of dilution of the alkaloids were performed by injecting identical volumes of same concentration of the alkaloids into the buffer. The area under each heat burst curve was determined by integration using the Origin 7.0 software to give the measure of the heat associated

with the injections. The heat associated with each alkaloid–buffer mixing was subtracted from the corresponding heat of alkaloid–DNA reactions to give the heat of the alkaloid–DNA binding. The heat of dilution of injecting the DNA into buffer alone was observed to be negligible. The resulting corrected injection heats were plotted as a function of the molar ratio, fit with a model for one set of binding sites, and analyzed using Origin 7.0 software to provide the binding affinity (K_a), the binding stoichiometry (N), and the enthalpy of binding (ΔH°). The binding free energy (ΔG°) and the entropic contribution to the binding ($T\Delta S^\circ$) were subsequently calculated from standard relationships described earlier.^{20a,23}

3. RESULTS AND DISCUSSION

3.1. Absorbance Spectral Studies and Evaluation of the Binding Affinities. Berberine and its 13-phenylalkyl analogues have characteristic absorption spectra in the 300–550 nm region that provide a convenient handle to monitor the DNA binding. Pronounced hypochromic and bathochromic effects were observed in the absorbance spectrum in this spectral region when the alkaloids were mixed with increasing concentrations of DNA, revealing strong intermolecular association. Such spectral changes have been usually ascribed to a strong interaction between the π electron cloud of the interacting ligand and the base pairs of DNA, presumably due to intercalation. Representative absorption spectra of the free and fully DNA bound BC and BC2 are presented in Figure 2A,B. The presence of sharp isosbestic points in each case enabled us to assume the existence of a two-state system consisting of bound and free alkaloids at any particular wavelength. A summary of the optical properties of the free and DNA bound analogues is presented (Table S1, Supporting Information). Titration of a constant concentration of DNA with increasing concentration of the analogues at several inputs was performed for evaluating the free and DNA bound alkaloid concentrations. Binding data obtained from spectrophotometric titration were cast into Scatchard plots of r/C_f versus r , where r is the number of moles of alkaloid bound per mole of DNA base pairs. In Figure 3A,B, the representative Scatchard plots of the binding of BC and BC3 to CT DNA are depicted. The binding isotherm of BC had positive slope at low r values, indicating cooperativity of binding while all the analogues had a negative slope. The substitution at the 13 position therefore changes the binding from cooperative to non-cooperative mode. Fitting of the isotherm of BC was therefore done using a theoretical curve drawn according to the excluded site model of McGhee and von Hippel for a cooperative ligand binding system (*vide supra*), while the curves of the analogues were fitted to the noncooperative equation. The binding data were analyzed using the Origin 7.0 software to determine the best-fit parameters of the intrinsic binding constant (K_i) to an isolated binding site where n is the number of base pairs excluded by the binding of a single alkaloid molecule and ω the cooperativity factor (for BC only). Cooperative isotherms have been observed previously for the binding of BC and 9-O- ω amino alkyl BC analogues to CT DNA.^{27,13b} The cooperative binding affinity (K_w) of BC to DNA was evaluated to be $1.03 \times 10^4 \text{ M}^{-1}$. The noncooperative binding affinity of the BC analogues and the number of excluded sites are depicted in Table 1. The apparent binding constant (K), a product of the cooperative binding affinity (K_w) and the cooperativity factor (ω) for the binding of BC, gave a value of $2.2 \times 10^5 \text{ M}^{-1}$. This value may be compared to the noncooperative binding affinity values of

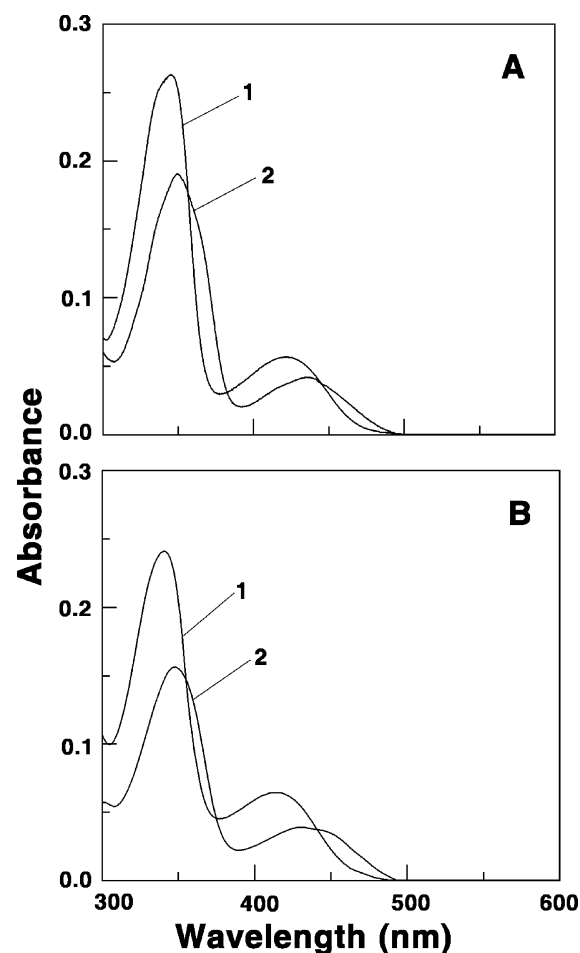


Figure 2. Absorption spectra of free (curve 1) and bound (curve 2) BC (A) and BC2 (B) in the presence of saturating concentrations of CT DNA in 10 mM CP buffer, pH 7.0, at 20 °C.

the analogues. It can be seen that the magnitude of the binding varied as $BC6 \cong BC5 \cong BC4 < BC3 > BC2 > BC > BC1$. Thus, beyond a length of $(CH_2)_3$, the DNA binding affinity decreased. The values of excluded sites for the analogues were in the range 3.2–3.8, except for BC1 for which a higher value of around 5.0 was obtained.

3.2. Fluorescence Titration Studies. Berberine is a weak fluorophore with an emission maximum around 444 nm when excited at 345 nm.^{6d,7} Substitution at the 13-position resulted in a small enhancement of the fluorescence emission intensity with large red shift of the emission maxima (Table S1, Supporting Information). For BC3, the maximum was around 506 nm, with a shift of about 60 nm compared to BC, indicating the weakening of the electronic structure of the ring. Binding to ds DNAs is known to result in many-fold enhancement of the fluorescence intensity of BC.^{6d,7} In a similar fashion, binding of the analogues also resulted in large enhancements of their intrinsic fluorescence (Figure S1, Supporting Information), eventually leading to saturation in each case. Large fluorescence change is indicative of strong association resulting from an effective overlap of the electronic cloud of the bound analogues with the DNA base pairs. This also proposes the location of the bound molecules to be in a hydrophobic environment similar to an intercalated state. The binding isotherms constructed revealed cooperative binding for berberine (not shown) and noncooperative binding for all six

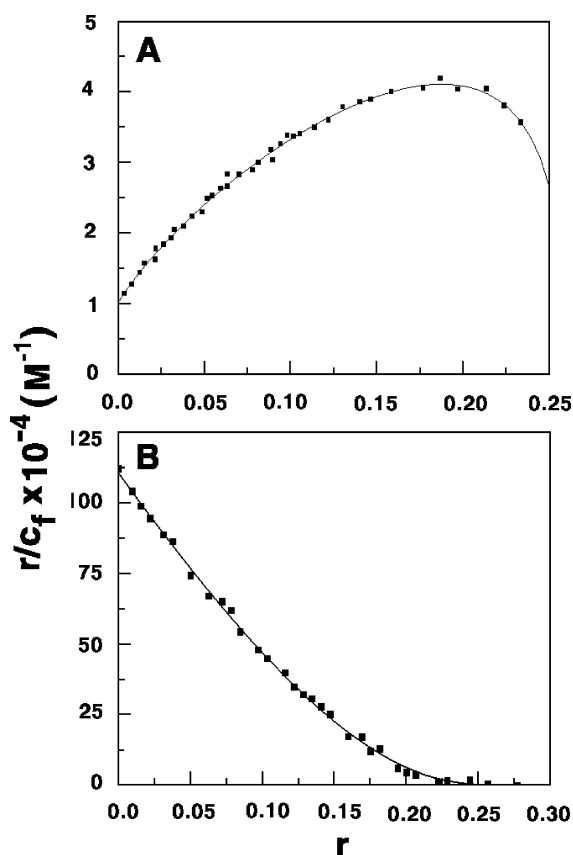


Figure 3. Scatchard plots for the binding of BC (A) and BC3 (B) to CT DNA obtained from spectrophotometric analysis. The solid lines represent the nonlinear least-squares best fit of the experimental points to the corresponding McGhee–von Hippel equations.

Table 1. Binding Parameters for the Association of Berberine Analogues with the CT DNA, Obtained from Spectroscopic Studies at 20 °C^a

analogue	spectrophotometry		spectrofluorimetry	
	$K_i \times 10^{-5} \text{ (M}^{-1}\text{)}$	n	$K_i \times 10^{-5} \text{ (M}^{-1}\text{)}$	n
BC1	0.35 ± 0.001	4.9	0.32 ± 0.002	5.2
BC2	2.11 ± 0.02	3.2	2.08 ± 0.02	3.1
BC3	11.01 ± 0.09	3.6	10.03 ± 0.08	3.8
BC4	7.60 ± 0.06	3.8	7.51 ± 0.07	3.9
BC5	7.58 ± 0.06	3.9	7.01 ± 0.05	4.0
BC6	6.80 ± 0.04	4.2	6.40 ± 0.09	4.5

^aAll the data in this table are averages of four determinations conducted in CP buffer of pH 7.0 at 20 °C. K_i is the intrinsic binding constant to an isolated site, and n is the number of base pairs excluded by the binding of an alkaloid.

analogues (Figure S2, Supporting Information) as observed from absorption spectral data. The binding constants calculated from the fluorescence data as per the Scatchard analysis, using the cooperative binding model of McGhee–von Hippel for BC and noncooperative model for the analogues, yielded binding affinity values (Table 1), which are in excellent agreement with the spectrophotometric results. Again, the K value for BC ($1.9 \times 10^5 \text{ M}^{-1}$) is of the same order as the K_i values for others, and the results are in agreement with the values evaluated by spectrophotometric analysis. The magnitude and variation of the n values were also similar to those obtained from absorption studies.

3.3. Binding Stoichiometry (Job Plot). For determining the stoichiometry, the ligand:DNA molar ratio was varied while the total molar concentration remained constant. The stoichiometry of binding was determined from the molar ratio where maximal binding was observed. The plot of difference fluorescence intensity (ΔF) at the wavelength maximum versus the mole fraction of BC/BC analogues (Figure S3, Supporting Information) revealed a single binding mode in each case. From the inflection point, $\chi_{\text{ligand}} = 0.17, 0.26, 0.22, 0.21, 0.20,$ and 0.19 for BC 1–6. Thus, the number of DNA base pairs bound per berberine analogue can be estimated to be around 4.80, 2.85, 3.55, 3.76, 4.0, and 4.26, respectively. For berberine, this value was 2.44. The values of stoichiometry are in good agreement with the number of excluded sites obtained from the McGhee–von Hippel analysis of the spectroscopic data (Table 1).

3.4. Fluorescence Quenching Studies and Elucidation of the Mode of Binding. The intercalative DNA binding mode of berberine has been unequivocally established from the recent X-ray studies.⁹ Thus, it may be presumed that these analogues also may intercalate to DNA. We probed the DNA binding mode of the analogues in comparison with berberine using ferrocyanide quenching experiments. This anionic quencher would not be able to penetrate the negatively charged double helix. Therefore, if these analogues are bound inside the DNA helix by intercalation, little or no change in fluorescence is expected. Stern–Volmer plots for the quenching of the fluorescence of BC analogues by the DNA are shown in Figure 4. The results clearly indicated that free molecules were

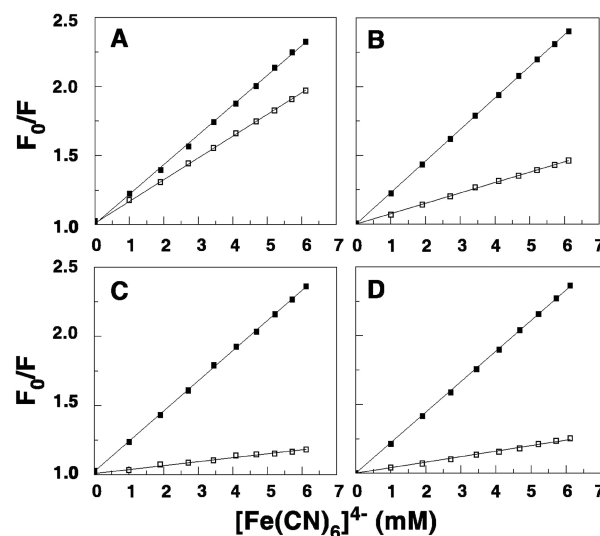


Figure 4. Stern–Volmer plots for quenching of fluorescence intensity by increasing concentration of $[\text{Fe}(\text{CN})_6]^{4-}$ of (A) BC1, (B) BC2, (C) BC3, and (D) BC4 in the absence (■) and in the presence (□) of CT DNA in 10 mM CP buffer, pH 7.0, at 20 °C.

quenched efficiently. More quenching was observed in the case of BC1 and less quenching for bound BC2–4, indicating that the bound analogues are, like berberine, located in a relatively more protected environment compared to the free molecules. The quenching constants (K_{sv}) calculated were in the range 215–230 M^{-1} for the unbound BC and analogues, and 91, 157, 75, 28, 40, 40, and 40 M^{-1} , respectively, for bound BC and BC1–6. From these results, it can be inferred that the bound alkaloid analogues are sequestered away from the solvent,

confirming strong intercalative binding. The trend in the values suggests that the K_{sv} of BC is lower than that of BC1 and for the others it varied as $BC6 \cong BC5 \cong BC4 > BC3 < BC2$. Thus, these data suggest that BC is better intercalated than BC1, and BC3 has a better intercalation capability compared to BC4, BC5, and BC6. This trend was also reflected from the spectral data. With BC1, the phenyl group is separated by one (CH_2) and appears to be too close to the berberine moiety, resulting in hindrance to the intercalation geometry. Furthermore, after a critical length of three CH_2 groups in the chain, the intercalation capability remained more or less the same. These conclusions were also supported by viscosity studies (Supporting Information) where length enhancement was maximum with BC3 (Figure S4, Supporting Information).

3.5. Optical Thermal Melting and Differential Scanning Calorimetric Studies. Strong binding of small molecules, particularly intercalation into DNA base pairs, causes stabilization of the base stacking, resulting in enhancement of the stability of the DNA helix. This in turn results in an enhancement of the melting temperature (T_m) that is easily revealed from optical melting (at $\lambda_{max} = 260$ nm) and differential scanning calorimetry experiments. The melting profiles of CT-DNA in the presence of saturating D/P (alkaloid/DNA base pair molar ratio) values of BC and BC1–4 are presented in Figure 5. The DNA itself exhibited a

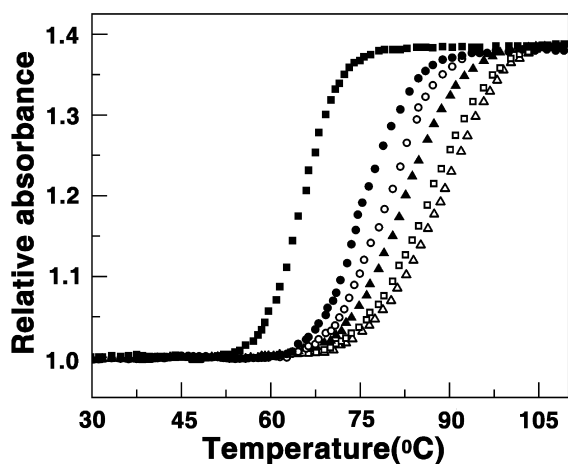


Figure 5. Thermal melting profiles (absorbance change at 260 nm versus temperature) of CT DNA (■) and its complexes with BC (○), BC1 (●), BC2 (▲), BC3 (△), and BC4 (□) at the respective saturation D/P values.

T_m of 65.0 °C under the conditions of this study, showing a cooperative transition with ~40% hyperchromicity. At saturating conditions (D/P = 1.0), BC stabilized the DNA by about 13.0 °C and BC1 by 10.0 °C, while BC2, BC3, BC4, BC5, and BC6 enhanced the T_m by 16, 23, 20, 19.5, and 19.0 °C, respectively. These data were further supported by DSC results (Figure S5, Supporting Information). Melting temperature data presented in Table 2 were also used to calculate the binding constants of the analogues to DNA using the equation derived by Crothers²⁸

$$1/T_m^\circ - 1/T_m = (R/n\Delta H_{wc}) \ln(1 + K_{Tm}\alpha) \quad (6)$$

where T_m° is the melting temperature of the DNA alone, T_m is the melting temperature in the presence of saturating amounts of the alkaloids, ΔH_{wc} is the enthalpy of DNA melting, R is the universal gas constant ($1.987 \text{ cal K}^{-1} \text{ mol}^{-1}$), K_{Tm} is the

Table 2. Optical Thermal Melting Data and Binding Constants Derived from Optical Melting Data at Saturating Concentrations of BC and Analogues with CT DNA^a

system	T_m (°C) (optical melting)	T_m (°C) (DSC)	ΔT_m	$K_{Tm} \times 10^{-5}$ (M^{-1})	$K_{obs} \times 10^{-5}$ (M^{-1})
DNA	65.0	65.0			
DNA +BC	78.0	79.0	13.5	0.772	1.77
DNA +BC1	75.0	75.0	10.0	0.587	0.465
DNA +BC2	81.0	82.0	16.5	1.424	2.72
DNA +BC3	88.0	88.0	23.0	7.73	10.30
DNA +BC4	85.0	86.0	20.0	5.08	8.35
DNA +BC5	84.5	nd	19.5	4.55	7.66
DNA +BC6	84.0	nd	19.0	4.82	7.64

^aMelting stabilization of DNA duplex in the presence of saturating amounts of the alkaloids in CP buffer of 10 mM $[Na^+]$, pH 7.0. The data are averages of four determinations. K_{Tm} is the binding constant at the melting temperature, and K_{obs} is the drug-binding constant at 20 °C calculated using eqs 6 and 7 described in the text.

alkaloid binding constant at T_m , α is the free alkaloid activity that may be estimated by one-half of the total alkaloid concentration, and n is the site size of the alkaloid binding. The calculated apparent binding constant at the melting temperature can be extrapolated to a reference temperature (say 20 °C) using the standard relationship

$$\delta[\ln(K_{obs})]/\delta(1/T) = -(\Delta H_b/R) \quad (7)$$

where K_{obs} is the drug binding constant at the reference temperature T (in kelvins) and ΔH_b is the binding enthalpy which was determined directly from the isothermal titration calorimetry experiment (vide infra). The binding constants (K_{obs}) calculated for 20 °C from these data are depicted in Table 2. These values are of the same order as and close to the values of K_i from spectroscopic studies. The values of K_{obs} were low for BC1, increased up to BC3, and then slightly decreased for BC4 and BC5. This result further confirms the importance of the optimum length of the CH_2 chain in the DNA interaction profile of these analogues.

3.6. Circular Dichroism Spectral Study. Having established that the BC analogues bind DNA strongly by intercalation, the conformational changes associated with the binding were investigated from circular dichroism studies. The CD spectra of the DNA duplex displayed a canonical B-form conformation characterized by a positive band in the 275–280 nm range and a negative band around 248 nm. These bands are caused due to the stacking interactions between the base pairs and the helical structure of the duplex that provides an asymmetric environment for the bases. Berberine and its analogues, on the other hand, do not have any intrinsic optical activity. However, they may acquire optical activity manifesting an induced CD on binding to helical organization of DNA.^{6b} To record the alkaloid-induced changes in the DNA conformation, the CD spectra in the 200–450 nm regions were recorded in the presence of varying D/P values. The comparative CD data for BC and BC3 are presented in Figure 6. The ellipticity of the long wavelength positive band increased as the interaction progressed, with a slight red shift in the

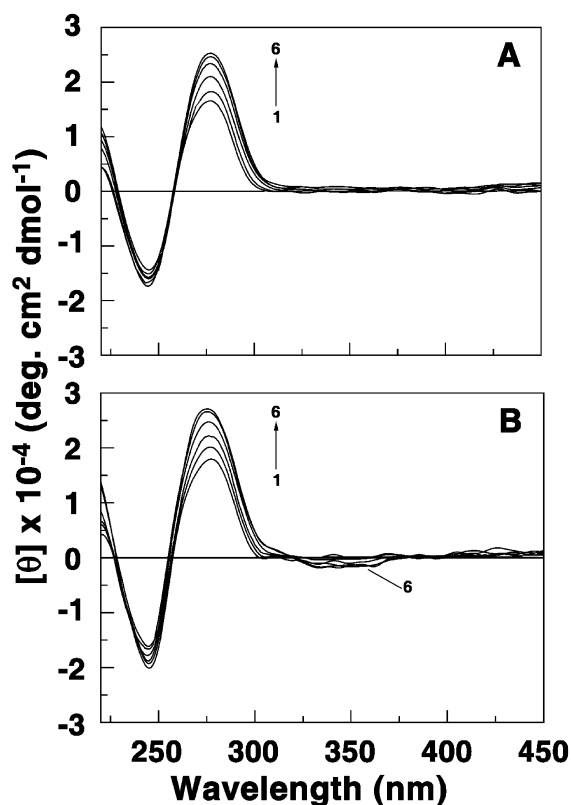


Figure 6. Representative CD spectra resulting from the interaction of BC and BC3 with CT DNA at pH 7.0 in citrate-phosphate buffer: (A) curves 1–6 denote CT DNA (30 μM) treated with 0, 6.0, 12.0, 18.0, 24.0, and 30.0 μM BC; (B) curves 1–6 denote CT DNA (30 μM) treated with 0, 6.0, 12.0, 18.0, 24.0, and 30.0 μM BC3.

wavelength maximum until saturation was achieved at a D/P of 1.0. There was not much change in the ellipticity of the negative 248 nm band. More detailed investigations on the induced CD for the bound alkaloid analogues in the range

300–500 nm were done, and the spectra are presented (Figure S6, Supporting Information). The results suggest that induced CD band ellipticity at 340 nm was highest with BC3 and thereafter reduced in intensity, in conformity with the results of other experiments.

3.7. Thermodynamics of the Interaction. Thermodynamic characterization of the binding of the BC analogues under investigation to the DNA was performed by isothermal titration calorimetry (ITC). It is an effective and sensitive tool to characterize the binding of small molecules to biomacromolecules and may provide key insights into the molecular forces that drive the complex formation.²⁹ The advantage of ITC is that from a single titration a complete thermodynamic profile of the interaction can be obtained along with the affinity constant of the binding and stoichiometry. The top panel of Figure 7 presents the representative primary data from the calorimetric titration of four BC analogues into a solution of CT DNA at 20 $^{\circ}\text{C}$. Each heat burst curve in the figures corresponds to that of a single injection. These injection heats were corrected by subtracting the corresponding dilution heats derived from the injection of identical amounts of alkaloid analogue into the buffer alone (shown at the top portion of the upper panel, curves offset for clarity). In the bottom panels of the figure, the resulting corrected heats are plotted against the molar ratio. The data points reflect the experimental points, and the continuous lines represent the calculated best fit to the data for the one-site model. The binding was characterized by exothermic heats in each case except with BC1, where it was endothermic. The ITC data were fit to a single-site model as the integrated heat data showed only one binding event. The results of the ITC experiments are presented in Table 3. We find an unusual positive enthalpy for the binding of BC1 to CT DNA but a negative one for those of the other analogues. A large entropy contribution was seen for the binding of BC1 compared to BC and BC2, and this may be interpreted in terms of binding-induced release of bound water and condensed sodium ions. The phenyl moiety is close to the berberine

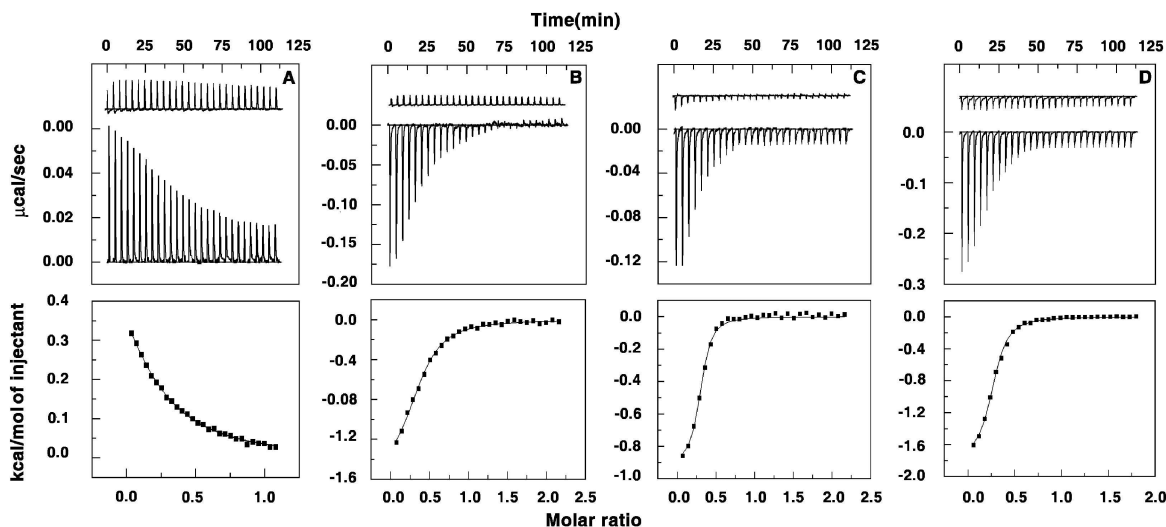


Figure 7. Representative ITC profiles for the titration of (A) BC1 (500 μM) into a 100 μM solution of CT DNA, (B) BC2 (500 μM) into a 50 μM solution of CT DNA, (C) BC3 (500 μM) into a 50 μM solution of CT DNA, and (D) BC4 (400 μM) into a 50 μM solution of CT DNA at 20 $^{\circ}\text{C}$. Each heat burst curve is the result of a 10 μL injection of BC analogues into the DNA solution. The upper part of panels A–D shows the heat burst curve for the injection of BC analogues into the buffer as control. The lower panels represent the corresponding normalized heat signals versus molar ratio. The data points (■) reflect the experimental injection heat, while the solid line represents the calculated fit of the data. The binding constants and other thermodynamic parameters are depicted in Table 3.

Table 3. Thermodynamic Parameters for the Association of Berberine and Analogues with CT DNA at 20 °C^a

analogue	$K_a \times 10^{-5} \text{ (M}^{-1}\text{)}$	n	$\Delta G^\circ \text{ (kcal/mol)}$	$\Delta H^\circ \text{ (kcal/mol)}$	$T\Delta S^\circ \text{ (kcal/mol)}$
BC	1.77 ± 0.07	1.92	-7.04 ± 0.15	-2.94 ± 0.039	4.10
BC1	0.31 ± 0.02	5.00	-6.04 ± 0.09	$+0.87 \pm 0.075$	6.91
BC2	2.07 ± 0.15	2.78	-7.13 ± 0.25	-1.59 ± 0.046	5.53
BC3	11.20 ± 0.8	3.57	-8.12 ± 0.41	-0.91 ± 0.019	7.21
BC4	7.60 ± 0.13	3.85	-7.89 ± 0.35	-1.79 ± 0.064	6.09
BC5	7.45 ± 0.64	4.00	-7.87 ± 0.18	-2.19 ± 0.041	5.68
BC6	6.85 ± 0.61	4.76	-7.83 ± 0.21	-1.56 ± 0.024	6.27

^aAll the data in this table are derived from ITC experiments conducted in CP buffer of 10 mM [Na⁺], pH 7.0, and are averages of four determinations. K_a and ΔH° values were determined from ITC profiles fitting to Origin 7 software as described in the text. The values of ΔG° and $T\Delta S^\circ$ were determined using the equations $\Delta G^\circ = -RT \ln K_a$ and $T\Delta S^\circ = \Delta H^\circ - \Delta G^\circ$. n is the site size which is the reciprocal of stoichiometry (N). All the ITC profiles were fit to a model of a single binding site.

chromophore, and hence, the binding results in close contact of the bulky phenyl with the base pairs and grooves. The closeness of the phenyl group to the isoquinoline chromophore also lowered the binding affinity due to steric effects in that BC1 probably is not able to fully intercalate into the DNA base pairs. The binding affinity values obtained from ITC are in the order of 10^5 M^{-1} for BC, BC2, and BC4–6. The affinity was 1 order lower for BC1 but of the order of 10^6 for BC3 and follows the same trend as that obtained from spectroscopic studies. A comparative bar chart of the binding affinities is presented in Figure 8. The site size of binding (n), which is the reciprocal of

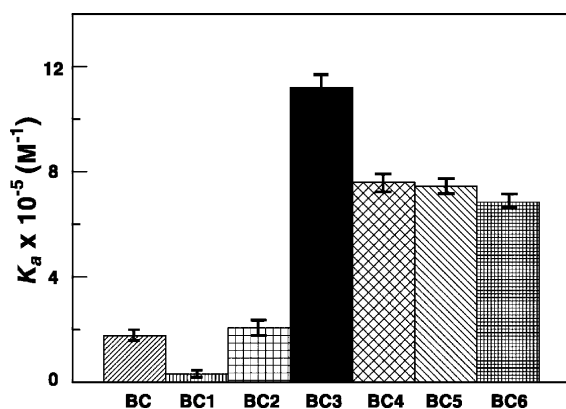


Figure 8. Bar chart showing comparative binding constants of BC and analogues with CT DNA.

stoichiometry (N), is comparable to the excluded sites from spectroscopy data. The binding of BC was driven largely by negative enthalpy and a larger favorable entropy change. The data on BC is similar to that reported previously.²⁷ The binding of BC2 was favored by a strong entropy contribution and a small enthalpy contribution. The strongest binding was observed for BC3, which was entropy driven ($T\Delta S^\circ = 7.21 \text{ kcal/mol}$) with an enthalpy contribution of only 0.91 kcal/mol . The bindings of BC4–6 were weaker compared to BC3 and were again favored by large entropy and relatively smaller enthalpy contributions as in the case of BC2. A bar diagram showing the variation of the thermodynamic parameters of BC and BC2–4 is presented in Figure 9. The trend observed here in the thermodynamic parameters is generally typical for intercalative interaction of small molecules to nucleic acids.^{30,31} The strong and dominating positive entropy term in each of the analogues compared to BC is suggestive of the disruption and release of water molecules on intercalation into the DNA double helix. The binding affinity values observed from ITC

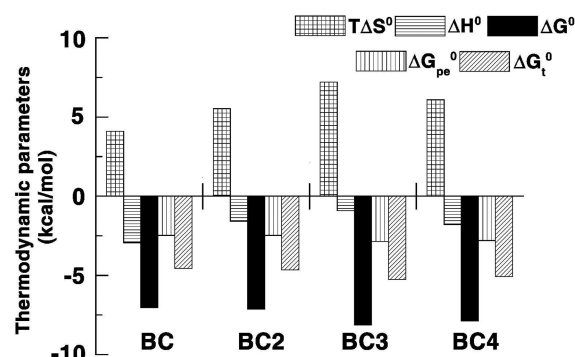


Figure 9. Comparative thermodynamic profiles of interaction of BC, BC2, BC3, and BC4 with CT DNA.

may be equated with K_i values from spectroscopy. It is noteworthy that these values are also comparable to the K_{obs} values evaluated from the melting data.

3.8. Dependence of Binding on the Ionic Strength of the Medium. Berberine analogues have a quaternary nitrogen atom that is positively charged. To provide insight into the nature of the binding, the effect of salt concentration on the binding in ITC was determined for BC2, BC3, and BC4 in conjunction with van't Hoff analysis. The following relation has been described previously,³² linking the binding constant with the [Na⁺] ion concentration.

$$\delta \log(K_a) / \delta \log([Na^+]) = -Z\psi \quad (8)$$

where Z is the apparent charge of the bound ligand and ψ is the fraction of [Na⁺] bound per DNA phosphate group. The slope of the plot of $\ln K$ versus $\ln [Na^+]$ gave values of -0.92 , -1.06 , and -1.04 , respectively, for BC2, BC3, and BC4. The observed free energies of the interaction were in the range 6.0 – 8.0 kcal/mol (Table 4). From the dependence of K_a on [Na⁺], the observed free energy can be partitioned between the polyelectrolytic (ΔG^{pe}) and non-polyelectrolytic (ΔG^{t}) contributions. The contribution to the free energy from the electrostatic interaction (polyelectrolytic) can be quantitatively determined from the relationship

$$\Delta G^{\text{pe}} = Z\psi RT \ln([Na^+]) \quad (9)$$

where $Z\psi$ is the slope of the van't Hoff plot. At $50 \text{ mM [Na}^+]$, the contributions to the ΔG^{pe} values have been determined to be around 1.61 , 1.86 , and 1.83 kcal/mol for BC2, BC3, and BC4 (Table 4), which are only about 25% of the total free energy change. This is similar to that observed with the binding of berberine, palmatine, and coralyne to ds DNA and dsRNAs,

Table 4. Thermodynamic Parameters for the Association of Berberine Analogues BC2, BC3, and BC4 with CT DNA at Different Salt Concentrations^a

analogue	[Na ⁺] (mM)	$K_a \times 10^{-5} \text{ (M}^{-1}\text{)}$	$\Delta H^\circ \text{ (kcal/mol)}$	$T\Delta S^\circ \text{ (kcal/mol)}$	$\Delta G^\circ \text{ (kcal/mol)}$	$\Delta G^{\circ\text{pe}} \text{ (kcal/mol)}$	$\Delta G^{\circ\text{t}} \text{ (kcal/mol)}$
BC2	10	2.07	−1.59	5.53	−7.13	−2.48	−4.65
	20	0.98	−1.47	5.21	−6.68	−2.11	−4.57
	50	0.47	−1.30	4.95	−6.25	−1.61	−4.64
BC3	10	11.20	−0.91	7.21	−8.12	−2.86	−5.26
	20	4.82	−0.78	6.82	−7.60	−2.43	−5.17
	50	2.00	−0.70	6.39	−7.09	−1.86	−5.23
BC4	10	7.65	−1.79	6.09	−7.88	−2.81	−5.07
	20	3.59	−1.50	5.94	−7.45	−2.38	−5.07
	50	1.41	−1.37	5.53	−6.95	−1.83	−5.08

^aAll the data in this table are derived from ITC experiments conducted in CP buffer of different [Na⁺], pH 7.0 and are averages of four determinations. K_a and ΔH° values were determined from ITC profiles fitting to Origin 7 software as described in the text. The values of ΔG° and $T\Delta S^\circ$ were determined using the equations $\Delta G^\circ = -RT \ln K_a$ and $T\Delta S^\circ = \Delta H^\circ - \Delta G^\circ$. All the ITC profiles were fit to a model of a single binding site.

where <25% of the free energy has been suggested to arise from polyelectrolytic forces.^{19b,27} At all salt concentrations, the ΔG° that had large magnitude in each case remained almost invariant. Thus, although positively charged like the parent alkaloid, the DNA binding of these analogues is dominated by forces other than electrostatic.

4. CONCLUSIONS

The structural aspects and thermodynamics of interaction of six 13-phenylalkyl substituted berberines with calf thymus DNA was studied in comparison with berberine. As the chain length of the substitution increased beyond CH₂, the affinity enhanced until the critical length of (CH₂)₃, after which the binding affinity decreased slightly. The highest binding affinity was for BC3 ($1.12 \times 10^6 \text{ M}^{-1}$) which was more than 6 times that of BC under identical conditions. The substitution enhanced the thermal stabilization of DNA remarkably. BC3 enhanced the stability 10 °C higher than BC, clearly suggesting strong additional binding effects from the side chain. Ferrocyanide quenching results and viscosity data conclusively proved stronger intercalative geometry for the analogues BC1–BC3 compared to BC, the best being BC3; the data also reflected the weakening of the binding beyond BC3. Moderate conformational changes of DNA within an overall B-form geometry have been observed, and the induced CD spectra showed remarkable changes indicated by the loss of the 430 nm band with concomitant strengthening of the rotational strength of the negative band around 350 nm. The thermodynamics of the interaction suggested an unfavorable nature of the effect of the phenyl group in proximity (in BC1) that became more favorable as the alkyl chain length increased, driven largely by entropy contributions in the case of BC3–6. In all the cases, the binding was dominated by nonelectrostatic forces that contributed to at least 75% of the binding free energy. This study proves that substitution at the 13-position of berberine remarkably enhanced the DNA binding action of BC and provided evidence that a threshold length of the side chain is critical for strong binding to occur. These results provide new insights into the 13-position substitution of berberine in enhancing the DNA binding that may be useful for the design and development of new drugs with higher efficacy.

■ ASSOCIATED CONTENT

● Supporting Information

A summary of the optical properties of the free and DNA bound BC analogues (Table S1); fluorescence spectral titration of berberine analogues with DNA (Figure S1); the Scatchard binding isotherms from fluorescence data (Figure S2); Job plots for the binding of BC and BC analogues to DNA (Figure S3); description of the viscosity studies and a plot of L/L_0 versus the molar ratio of the alkaloids (Figure S4); DSC profiles of BC and BC analogues complexed with DNA (Figure S6); results of induced CD studies and the induced CD spectra of BC and analogues complexing with CT DNA (Figure S5). This material is available free of charge via the Internet at <http://pubs.acs.org>.

■ AUTHOR INFORMATION

Corresponding Author

*Address: Biophysical Chemistry Laboratory, Chemistry Division, Indian Institute of Chemical Biology (CSIR, Govt. of India), 4, Raja S. C. Mullick Road, Jadavpur, Kolkata 700 032, India. Phone: +91 33 2472 4049/2499 5723. Fax: +91 33 2472 3967. E-mail: gskumar@iicb.res.in/gsk.iicb@gmail.com.

Notes

The authors declare no competing financial interest.

■ ACKNOWLEDGMENTS

D.B. acknowledges financial assistance in the form of NET-Junior Research Fellowship from the University Grants Commission, Govt. of India. M.H. thanks Council of Scientific and Industrial Research, Govt. of India, for the award of Research Associateship. This work was partially funded by grants from the CSIR network project NWP0036 on “comparative genomics and biology of non coding RNA in the human genome”. The authors are grateful to Dr. Basudeb Achari, Scientist (Retd.), CSIR-IICB, for the critical reading of the manuscript and all the colleagues of the Biophysical Chemistry Laboratory for help and cooperation at every stage of this work. Naxospharma srl, Italy, acknowledges financial support by the Italian Ministry of Economic Development, Grant No. 01467, awarded within the third Call of the EuroTransBio initiative. The critical comments of the anonymous reviewers that enabled us to improve the manuscript are also highly appreciated.

REFERENCES

- (1) (a) Grycová, L.; Dostál, J.; Marek, R. *Phytochemistry* **2007**, *68*, 150–175. (b) Küpeli, E.; Koşar, M.; Yeşilada, E.; Başer, K. H. C.; Başer, C. *Life Sci.* **2002**, *72*, 645–657. (c) Iwasa, K.; Moriyasu, M.; Tachibana, Y.; Kim, H.-S.; Wataya, Y.; Wiegerebe, W.; Bastow, K. F.; Cosentino, L. M.; Kozuka, M.; Lee, K.-H. *Bioorg. Med. Chem.* **2001**, *9*, 2871–2884. (d) Nafisi, S.; Malekabad, Z. M.; Khalilzadeh, M. A. *DNA Cell Biol.* **2010**, *29*, 753–761. (e) Nafisi, S.; Bonsaii, M.; Maali, P.; Khalilzadeh, M. A.; Manouchehri, F. *J. Photochem. Photobiol., B* **2010**, *100*, 84–91.
- (2) (a) Yin, J.; Xing, H.; Ye, J. *Metabolism* **2008**, *57*, 712–717. (b) Imanshahidi, M.; Hosseinzadeh, H. *Phytother. Res.* **2008**, *22*, 999–1012. (c) Cui, H.-S.; Hayasaka, S.; Zhang, X.-Y.; Hayasaka, Y.; Chi, Z.-L.; Zheng, L.-S. *Jpn. J. Ophthalmol.* **2007**, *51*, 64–67. (d) Choi, B.-H.; Ahn, I.-S.; Kim, Y.-H.; Park, J.-W.; Lee, S.-Y.; Hyun, C.-K.; Do, M.-S. *Exp. Mol. Med.* **2006**, *38*, 599–605. (e) Kuo, C. L.; Chi, C. W.; Liu, T. Y. *Cancer Lett.* **2004**, *203*, 127–137. (f) Pasqual, M. S.; Lauer, C. P.; Moyna, P.; Henriques, J. A. *Mutat. Res.* **1993**, *286*, 243–252. (g) Chiou, W.-F.; Yen, M.-H.; Chen, C.-F. *Eur. J. Pharmacol.* **1991**, *204*, 35–40. (h) Hui, K. K.; Yu, J. L.; Chan, W. F.; Tse, E. *Life Sci.* **1991**, *49*, 315–324. (i) Creasey, W. A. *Biochem. Pharmacol.* **1979**, *28*, 1081–1084.
- (3) (a) Amin, A. H.; Subbiah, T. V.; Abbasi, K. M. *Can. J. Microbiol.* **1969**, *15*, 1067–1076. (b) Stermitz, F. R.; Lorenz, P.; Tawara, J. N.; Zenewicz, L. A.; Lewis, K. *Proc. Natl. Acad. Sci. U.S.A.* **2000**, *97*, 1433–1437. (c) Cernakova, M.; Kostalova, D. *Folia Microbiol.* **2002**, *47*, 375–378. (d) Yu, H.-H.; Kim, K.-J.; Cha, J.-D.; Kim, H.-K.; Lee, Y.-E.; Choi, N.-Y.; You, Y.-O. *J. Med. Food Winter* **2005**, *8*, 454–461.
- (4) (a) Choi, M. S.; Oh, J. H.; Kim, S. M.; Jung, H. Y.; Yoo, H. S.; Lee, Y. M.; Moon, D. C.; Han, S. B.; Hong, J. T. *Int. J. Oncol.* **2009**, *34*, 1221–1230. (b) Letasiova, S.; Jantova, S.; Cipak, L.; Muckova, M. *Cancer Lett.* **2006**, *239*, 254–262. (c) Yang, I. W.; Chou, C. C.; Yung, B. Y. M. *Pharmacology* **1996**, *354*, 102–108. (d) Kuo, C. L.; Chou, C. C.; Yung, B. Y. M. *Cancer Lett.* **1995**, *93*, 193–200.
- (5) (a) Wartenberg, M.; Budde, P.; De Marees, M.; Grunheck, F.; Tsang, S. Y.; Huang, Y.; Chen, Z. Y.; Hescheler, J.; Sauer, H. *Lab. Invest.* **2003**, *83*, 87–98. (b) Iizuka, N.; Miyamoto, K.; Okita, K.; Tangoku, A.; Hayashi, H.; Yosino, S.; Abe, T.; Morioka, T.; Hazama, S.; Oka, M. *Cancer Lett.* **2000**, *148*, 19–25. (c) Mantena, S. K.; Sharma, S. D.; Katyar, S. K. *Mol. Cancer Ther.* **2006**, *5*, 296–308. (d) Lin, J.-P.; Yang, J.-S.; Lee, J.-H.; Hsieh, W.-T.; Chung, J.-G. *World J. Gastroenterol.* **2006**, *12*, 21–28. (e) Peng, P. L.; Hsieh, Y. S.; Wang, C. J.; Hsu, J. L.; Chou, F. P. *Toxicol. Appl. Pharmacol.* **2006**, *214*, 8–15. (f) Kim, J. B.; Lee, K. M.; Ko, E.; Han, W.; Lee, J. E.; Shin, I.; Bae, J. Y.; Kim, S.; Noh, D. Y. *Planta Med.* **2008**, *74*, 39–42. (g) Ho, Y. T.; Yang, J. S.; Lu, C. C.; Chiang, J. H.; Li, T. C.; Lin, J. J.; Lai, K. C.; Liao, C. L.; Lin, J. G.; Chung, J. G. *Phytomedicine* **2009**, *16*, 887–890. (h) Sun, Y.; Xun, K.; Wang, Y.; Chen, X. *Anticancer Drugs* **2009**, *20*, 757–769. (i) Mahata, S.; Bharti, A. C.; Shukla, S.; Tyagi, A.; Husain, S. A.; Das, B. C. *Mol. Cancer* **2011**, *10*, 39–52.
- (6) (a) Davidson, M. W.; Lopp, I.; Alexander, S.; Wilson, W. D. *Nucleic Acids Res.* **1977**, *4*, 2697–2712. (b) Debnath, D.; Suresh Kumar, G.; Maiti, M. *J. Biomol. Struct. Dyn.* **1991**, *9*, 61–79. (c) Saran, A.; Srivastava, S.; Coutinho, E.; Maiti, M. *Indian J. Biochem. Biophys.* **1995**, *32*, 74–77. (d) Krishnan, P.; Bastow, K. F. *Anti-Cancer Drug Des.* **2000**, *15*, 255–264. (e) Li, T. K.; Bathory, E.; LaVoie, E. J.; Srinivasan, A. R.; Olson, W. K.; Sauers, R. R.; Liu, L. F.; Pilch, D. S. *Biochemistry* **2000**, *39*, 7107–7116. (f) Bhadra, K.; Suresh Kumar, G.; Das, S.; Islam, M. M.; Maiti, M. *Bioorg. Med. Chem.* **2005**, *13*, 4851–4856. (g) Wang, Y.; Kheir, M. M.; Chai, Y.; Hu, J.; Xing, D.; Lei, F.; Du, L. *PLoS ONE* **2011**, *6*, e23495. (h) Maiti, M.; Suresh Kumar, G. *Med. Res. Rev.* **2007**, *27*, 649–695. (i) Qina, Y.; Pang, J. Y.; Chen, W. H.; Zhao, Z. Z.; Liu, L.; Jiang, Z. H. *Chem. Biodiversity* **2007**, *4*, 481–487. (j) Bhadra, K.; Suresh Kumar, G. *Med. Res. Rev.* **2011**, *31*, 821–862.
- (7) (a) Debnath, D.; Suresh Kumar, G.; Nandi, R.; Maiti, M. *Indian J. Biochem. Biophys.* **1989**, *26*, 201–208. (b) Bhadra, K.; Maiti, M.; Suresh Kumar, G. *Biochim. Biophys. Acta* **2008**, *1780*, 1054–1061.
- (8) (a) Li, W. Y.; Lu, H.; Xu, C. X.; Zhang, J. B.; Lu, Z. H. *Spectrosc. Lett.* **1998**, *31*, 1287–1298. (b) Mazzini, S.; Bellucci, M. C.; Mondelli, R. *Bioorg. Med. Chem.* **2003**, *11*, 505–514.
- (9) Ferraroni, M.; Bazzicalupi, C.; Bilia, A. R.; Gratter, P. *Chem. Commun.* **2011**, *47*, 4917–4919.
- (10) (a) Naasani, I.; Seimiya, H.; Yamori, T.; Tsuruo, T. *Cancer Res.* **1999**, *59*, 4004–4011. (b) Franceschini, M.; Rossetti, L.; D'Ambrosio, A.; Schirripa, S.; Bianco, A.; Ortaggi, G.; Savino, M.; Schultes, C.; Neidle, S. *Bioorg. Med. Chem. Lett.* **2006**, *16*, 1707–1711. (c) Zhang, W. J.; Ou, T. M.; Lu, Y. J.; Huang, Y. Y.; Wu, W. B.; Huang, Z. S.; Zhou, J. L.; Wong, K. Y.; Gu, L. Q. *Bioorg. Med. Chem.* **2007**, *15*, 5493–5501. (d) Gornall, K. C.; Samosorn, S.; Tanwirat, B.; Suksamrarn, A.; Bremner, J. B.; Kelso, M. J.; Beck, J. L. *Chem. Commun.* **2010**, *46*, 6602–6604.
- (11) (a) Iwasa, K.; Kamiguchi, M.; Ueki, M.; Taniguchi, M. *Eur. J. Med. Chem.* **1996**, *31*, 469–478. (b) Iwasa, K.; Nanba, H.; Lee, D. U.; Kang, S. I. *Planta Med.* **1998**, *64*, 748–751. (c) Lee, D. U.; Kang, Y. J.; Park, M. K.; Lee, Y. S.; Seo, H. G.; Kim, T. S.; Kim, C. H.; Chang, K. C. *Life Sci.* **2003**, *73*, 1401–1412.
- (12) (a) Park, K. D.; Lee, J. H.; Kim, S. H.; Kang, T. H.; Moona, J. S.; Kim, S. U. *Bioorg. Med. Chem. Lett.* **2006**, *16*, 3913–3916. (b) Samosorn, S.; Tanwirat, B.; Muhamad, N.; Casadei, G.; Tomkiewicz, D.; Lewis, K.; Suksamrarn, A.; Pramananan, T.; Gornall, K. C.; Beck, J. L.; Bremner, J. B. *Bioorg. Med. Chem.* **2009**, *17*, 3866–3872.
- (13) (a) Cui, J. S.; Xu, F.; Pang, J. Y.; Chen, W. H.; Jiang, Z. H. *Chem. Biodiversity* **2010**, *7*, 2908–16. (b) Islam, M. M.; Basu, A.; Hossain, M.; Suresh Kumar, G.; Hotha, S.; Suresh Kumar, G. *DNA Cell Biol.* **2011**, *30*, 123–133.
- (14) Islam, M. M.; Basu, A.; Suresh Kumar, G. *Med. Chem. Commun.* **2011**, *2*, 631–637.
- (15) Samosorn, S.; Tanwirat, B.; Muhamad, N.; Casadei, G.; Tomkiewicz, D.; Lewis, K.; Suksamrarn, A.; Pramananan, T.; Gornall, K. C.; Beck, J. L.; Bremner, J. B. *Bioorg. Med. Chem.* **2009**, *17*, 3866–3872.
- (16) (a) Iwasa, K.; Moriyasu, M.; Yamori, T.; Tsuruo, T.; Lee, D. U. *J. Nat. Prod.* **2001**, *64*, 896–898. (b) Gornall, K. C.; Samosorn, S.; Tanwirat, B.; Suksamrarn, A.; Bremner, J. B.; Kelso, M. J.; Beck, J. L. *Chem. Commun.* **2010**, *46*, 6602–6604.
- (17) Naxospharma srl, US Patent appl. US 12/458,657, filed July 20, 2009; published as US 2011/015222 A1 on January 20, 2011.
- (18) Chaires, J. B. *Biochemistry* **1983**, *22*, 4204–4211.
- (19) (a) Bhadra, K.; Maiti, M.; Suresh Kumar, G. *Biochim. Biophys. Acta* **2007**, *1770*, 1071–1080. (b) Islam, M. M.; Roy Chowdhury, S.; Suresh Kumar, G. *J. Phys. Chem. B* **2009**, *113*, 1210–1224.
- (20) (a) Sinha, R.; Islam, M. M.; Bhadra, K.; Suresh Kumar, G.; Banerjee, A.; Maiti, M. *Bioorg. Med. Chem.* **2006**, *14*, 800–814. (b) Islam, M. M.; Sinha, R.; Suresh Kumar, G. *Biophys. Chem.* **2007**, *125*, 508–520.
- (21) McGhee, J. D.; von Hippel, P. H. *J. Mol. Biol.* **1974**, *86*, 469–489.
- (22) (a) Job, P. *Ann. Chim.* **1928**, *9*, 113–203. (b) Huang, C. Y. *Methods Enzymol.* **1982**, *87*, 509–525.
- (23) Giri, P.; Suresh Kumar, G. *Arch. Biochem. Biophys.* **2008**, *474*, 183–192.
- (24) (a) Giri, P.; Suresh Kumar, G. *Mol. Biosyst.* **2008**, *4*, 341–348. (b) Islam, M. M.; Pandya, P.; Kumar, S.; Suresh Kumar, G. *Mol. Biosyst.* **2009**, *5*, 244–254. (c) Sinha, R.; Suresh Kumar, G. *J. Phys. Chem. B* **2009**, *113*, 13410–13420.
- (25) Müller, W.; Crothers, D. M. *J. Mol. Biol.* **1968**, *35*, 251–290.
- (26) Islam, M. M.; Pandya, P.; Roy Chowdhury, S.; Kumar, S.; Suresh Kumar, G. *J. Mol. Struct.* **2008**, *891*, 498–507.
- (27) Bhadra, K.; Maiti, M.; Suresh Kumar, G. *DNA Cell Biol.* **2008**, *27*, 675–685.
- (28) Crothers, D. M. *Biopolymers* **1968**, *6*, 575–584.
- (29) (a) O'Brien, R.; Haq, I. In *Applications of Biocalorimetry: Binding, Stability and Enzyme Kinetics*; Ladbury, J. E., Doyle, M., Eds.; Biocalorimetry 2; John Wiley and Sons Ltd: Chichester, U.K., 2004; pp 1–34. (b) Buurma, N. J.; Haq, I. *Methods* **2007**, *42*, 162–172.

- (c) Matthew, W. F.; Edwin, A. L. *Methods Cell. Biol.* **2008**, *84*, 79–113.
- (d) Bhadra, K.; Suresh Kumar, G. *Mini Rev. Med. Chem.* **2010**, *10*, 1235–1247.
- (30) (a) Haq, I. *Arch. Biochem. Biophys.* **2002**, *403*, 1–15. (b) Chaires, J. B. *Arch. Biochem. Biophys.* **2006**, *453*, 26–31. (c) Hossain, M.; Suresh Kumar, G. *Mol. BioSyst.* **2009**, *5*, 1311–1322. (d) Saha, I.; Hossain, M.; Suresh Kumar, G. *Phys. Chem. Chem. Phys.* **2010**, *12*, 12771–12779.
- (31) Chaires, J. B. *Ann. Rev. Biophys.* **2008**, *37*, 135–151.
- (32) Record, M. T. Jr; Anderson, C. F.; Lohman, T. M. *Q. Rev. Biophys.* **1978**, *11*, 103–178.